Predominance of allochthonous and refractory carbon in sediments from two contrasting Mexican mangrove ecosystems

J.L.J. Jupin, M. Boussafir, Abdel Sifeddine, A.C. Ruiz-Fernández, J.A. Sanchez-Cabeza, L.H. Pérez-Bernal

Catena 245 (2024) 108279

Contents lists available at ScienceDirect

Catena

journal homepage: www.elsevier.com/locate/catena

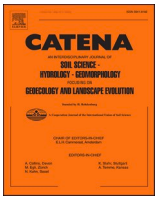

Predominance of allochthonous and refractory carbon in sediments from two contrasting Mexican mangrove ecosystems

J.L.J. Jupin [a,b], M. Boussafir [c], A. Sifeddine [b], A.C. Ruiz-Fernández [d,*], J.A. Sanchez-Cabeza [d], L. H. Pérez-Bernal [d]

[a] Posgrado en Ciencias del Mar y Limnología, Universidad Nacional Autónoma de México. Av. Universidad 3000, Ciudad Universitaria, Coyoacán, 04510, Ciudad de México, Mexico
[b] IRD, CNRS, SU, MNHN, IPSL, LOCEAN, Laboratoire d'Océanographie et du Climat : Expérimentation et Approches Numériques Centre IRD France Nord, 93143 Bondy, France
[c] Université de Tours, UR 6293, Géo-Hydrosystèmes Continentaux, Faculté des Sciences et Techniques, Parc de Grandmont, 37200 Tours, France
[d] Unidad Académica Mazatlán, Instituto de Ciencias del Mar y Limnología, Universidad Nacional Autónoma de México, 82040 Mazatlán, Sin., Mexico

ARTICLE INFO

Keywords:
Blue carbon
Organic carbon
Organic matter
Climate change
Mangroves
Rock-Eval
Palynofacies
Coastal lagoon
Ramsar

ABSTRACT

Mangroves are one of the most Blue Carbon-rich ecosystems worldwide, as they are highly efficient at storing and sequestering a large amount of organic carbon (C_{org}). The degradation of C_{org} inventories in mangrove sediments could cause carbon dioxide (CO_2) emissions, contributing to atmospheric warming. In this study, we used Rock-Eval pyrolysis and palynofacies identification to explore the composition and sources of organic matter (OM) and the quantity and liability of C_{org} in four ^{210}Pb-dated sediment cores from contrasting Mexican mangrove areas. The composition of terrestrial and refractory OM was similar in all cores, with variations attributed to the influence of the local river discharges on OM inputs and preservation. A progressive decrease in C_{org} quantity and lability from 2021 to 1990 in some cores was attributed to early diagenesis. Past precipitation and river discharge events appeared to have influenced carbon accumulation and preservation: increased influx and preservation of labile C_{org} in the sediments occurred during low river discharge and precipitation, whereas larger inputs and oxidation of refractory C_{org} occurred during high river discharge and precipitation. Sedimentary C_{org} stocks, assessed for 1921–2021, were primarily composed of refractory organic components, with degradation of allochthonous and autochthonous C_{org} mainly occurring before sediment burial. Sediments acted as efficient and long-term sinks for the C_{org} supplied to these mangroves, particularly in the context of increasing C_{org} inputs caused by an acceleration since the 1950s in continental erosion.

1. Introduction

Mangroves are considered high-priority ecosystems for large-scale international conservation efforts due to their high efficiency in storing Blue Carbon (i.e., carbon stored in coastal vegetated ecosystems), particularly in the context of climate change (Alongi, 2020; Friess et al., 2020). Those shrub-and-tree-dominated, intertidal, and salt-tolerant communities are important in the carbon cycle at local and global scales, owing to their (i) high primary production enhanced by nutrient trapping and recycling (Holguin et al., 2001); (ii) high organic carbon (C_{org}) accumulation from autochthonous (*in situ* litter and root production) and allochthonous inputs from adjacent habitats (Donato et al., 2011), and (iii) low rates of C_{org} decomposition due to suboxic to anoxic conditions (Alongi, 2005). The accumulation and preservation of C_{org} in mangrove ecosystems can exhibit high spatial and temporal variability, influenced by environmental settings (e.g., tidal, riverine, or wave-dominated), mangrove community structure, source and fluxes of allochthonous and autochthonous C_{org}, efficiency of C_{org} degradation during early diagenesis, and sediment accumulation rates (Woodroffe et al., 2005; Rovai et al., 2018).

While the majority of studies provide evidence that many mangrove forests effectively act as long-term sinks of atmospheric carbon dioxide (CO_2) and mitigate climate change (e.g., Bouillon et al., 2008; Kristensen et al., 2008), they may also be a source of greenhouse gases to the

* Corresponding author
E-mail addresses: johanna.jupin@ird.fr (J.L.J. Jupin), mohammed.boussafir@univ-tours.fr (M. Boussafir), abdel.sifeddine@ird.fr (A. Sifeddine), caro@ola.icmyl.unam.mx (A.C. Ruiz-Fernández), jasanchez@cmarl.unam.mx (J.A. Sanchez-Cabeza), lbernal@ola.icyml.unam.mx (L.H. Pérez-Bernal).

https://doi.org/10.1016/j.catena.2024.108279
Received 9 April 2024; Received in revised form 24 July 2024; Accepted 4 August 2024
Available online 14 August 2024

atmosphere (e.g., Borges et al., 2003; Rosentreter et al., 2018), in particular CO_2 and methane (CH_4) emissions coming from the surrounding waters (Bouillon et al., 2003; Koné and Borges, 2008). This apparent discrepancy can be attributed to the complex and dynamic nature of C_{org} accumulation and degradation processes (Rosentreter et al., 2018). This must be clarified since the role of mangroves as either sinks or sources of atmospheric CO_2 is fundamental in formulating effective strategies for mitigating climate change (Murdiyarso et al., 2015).

Rock-Eval® pyrolysis is a rapid and cost-effective method for determining the organic matter (OM) content of samples, including both organic and inorganic carbon fractions. The temperature-programmed pyrolyzer identifies OM sources, maturation types, and stages in diverse environments, such as soil (e.g., Sebag et al., 2016; Le Meur et al., 2021), recent lake sediments (e.g., Boussafir et al., 2012; Zhang et al., 2023), marine sediments (e.g., Baudin et al., 2015 and references therein), and mangrove sediments (e.g., Duan et al., 2020; Marchand et al., 2008). Rock-Eval can serve as a simulation of the natural OM decomposition during early diagenesis in sediments (Disnar, 1994; Williams and Rosenheim, 2015) and facilitates the determination of variations in OM stability over depth, time, and across different sites. The stability of OM is revealed through its resistance to thermal cracking during the Rock-Eval pyrolysis (Disnar et al., 2003), with higher temperature resistance indicating greater stability of the organic material and its 'refractory', 'recalcitrant' or 'resistant' character. Conversely, thermally labile OM is generally composed of readily decomposable organic compounds that can be rapidly removed during the earliest stages of diagenesis.

The complex interplay of factors, such as the variability of biological sources and soil environments, can challenge the interpretation of the Rock-Eval results (Disnar et al., 2003; Baudin et al., 2015). To address this, palynofacies analysis has commonly been used to complement Rock-Eval analyses of soil and sediment samples from continental, marine, and coastal environments (e.g., Sebag et al., 2006 and references therein), as it identifies and quantifies OM particles according to their source (terrestrial or aquatic), characteristics (biogenic, anthropogenic, or fossil), and formation process (biodegradation, oxidation, or combustion) (Combaz, 1964; Tyson, 1995).

Rock-Eval parameters and palynofacies analysis were used to determine C_{org} quantity and stability, and OM origin and composition in mangrove sediments from Términos Lagoon (TL) in the southern Gulf of Mexico and the El Verde Camacho Lagoon (EV) in the entrance of the Gulf of California. The Ramsar Convention recognizes TL and EV as wetlands of international importance (RSIS, 2024), as they exhibit rich biodiversity and serve as critical breeding grounds for numerous coastal species (Briseño-Dueñas, 2003; Venegas-Pérez, 2003). Despite higher precipitation, freshwater discharge, and land-use changes observed in TL compared to EV, a previous study on seven lead-210 (^{210}Pb) dated cores collected from mangrove sediments in both regions revealed a consistent century-long increase in sediment accumulation rates across all cores (Jupin et al., 2023).

In this study, four cores were re-examined with the hypotheses that site-specific characteristics would reflect differences in C_{org} origin, storage, and preservation within the mangrove ecosystems and that increasing sediment accumulation in the study sites may have induced a shift from autochthonous- to allochthonous-dominated C_{org} storage, thereby reducing the lability of sedimentary C_{org} stocks over time. The main questions addressed here were: (1) are the C_{org} quantity and stability and the OM origin and composition different among sites?; (2) what is the evolution of quantity and stability of the sedimentary C_{org} over the past century?; and (3) are these mangrove sediments a sink or a source of atmospheric CO_2?

2. Study sites

Términos Lagoon (TL), in the southern Gulf of Mexico, is Mexico's largest coastal lagoon (Fig. 1A). It is directly connected to the ocean via inlets on either side of Carmen Island, allowing a continuous influx of marine water into the lagoon. Most of the water that enters TL is fresh water from the Palizada River (9.08×10^9 m^3 yr^{-1}) and the Candelaria River discharge (1.6×10^9 m^3 yr^{-1}) (Fichez et al., 2017). The Palizada-del-Este (PDE) system, in the western TL zone, is the eastern part of the Grijalva-Usumacinta fluvial system, the largest river basin in Mexico; it has well-mixed conditions, low-salinity waters, and fine sediments. The climate is warm humid with an average annual temperature of 27 °C and abundant summer rains, averaging 1800 mm yr^{-1} (Bach et al., 2005; Yáñez-Arancibia and Day, 2005). In the eastern TL zone, the Candelaria-Panlau (CP) system has shallow lagoons and calcareous sediments, typical of the Yucatán calcareous peninsula. The climate of this eastern zone is warm sub-humid, with an average annual temperature of 27 °C and precipitation of 1400 mm yr^{-1}.

El Verde Camacho Lagoon (EV) is a 47-hectare internal coastal barrier lagoon (Fig. 1B), closed for most of the year but receiving marine water during the rainy season (June to October) when the sandbar is broken by the combined effects of the Quelite River water flow (0.11×10^9 m^3 yr^{-1}), high tides, and occasional tropical storms and hurricanes (Flores-Verdugo et al., 1995). The climate in the area is sub-humid tropical (García, 1973), with an average temperature of 25 °C and contrasting seasons. Depending on the sandbar status (open or closed) and the quantity of precipitation, averaging 750 mm yr^{-1} and falling mainly during the rainy season, the average salinity varies from 10 to 30 (CONAGUA, 2015).

3. Materials and methods

3.1. Sampling and dating

The four sediment cores were previously used for the evaluation of temporal variations in sediment accumulation in TL and EV, exploring how site characteristics (e.g., climate and anthropic activity) have influenced these trends over the past century; procedures for sampling and ^{210}Pb dating of the cores are detailed in Jupin et al. (2023). Briefly, four sediment push cores were collected by inserting PVC tubes (10 cm internal diameter, 1 m length) into the sediments of fringe mangrove communities (Fig. 1). The cores were extruded and sectioned every 1 cm, and samples were freeze-dried and ground to a powder. Age models and mass accumulation rates (MAR) were determined through the ^{210}Pb dating method using the Constant Flux model (Robbins, 1978; Sanchez-Cabeza and Ruiz-Fernández, 2012) and the radionuclide data (^{210}Pb, ^{226}Ra, and ^{137}Cs) obtained by gamma-ray spectrometry, as described in Díaz-Asencio et al., (2020). Sediment records spanned from 90 to 120 years, and MAR values varied from 0.03 ± 0.01 to 0.7 ± 0.6 g cm^{-2} yr^{-1} (Jupin et al., 2023).

3.2. Rock-Eval analysis

3.2.1. Concept and parameters

The composition and origin of OM and the concentration of C_{org} in the sediment samples were determined using a Rock-Eval 6® analyzer (Vinci Technologies™). About 60 mg of homogenized bulk sediment samples were analyzed by a pyrolysis program adapted for recent sediments, including two successive stages performed with heating rates of 30 °C min^{-1} (Baudin et al., 2015). It started with a sample pyrolysis (200–650 °C) under inert gas (helium), followed by an oxidation of the residual carbon (400–650 °C) under purified air. During the sequential program, the release of hydrocarbons (HC), carbon monoxide (CO), and CO_2 is continuously measured and reported in pyrograms; in particular, the S2 pyrogram corresponds with the quantity of HC compounds produced during the pyrolysis. The method's precision was determined by analyzing 20 sample duplicates; the coefficients of variation were < 4 % across the parameters and sediment cores.

Standard Rock-Eval parameters (Espitalié et al., 1977, 1985a, 1985b;

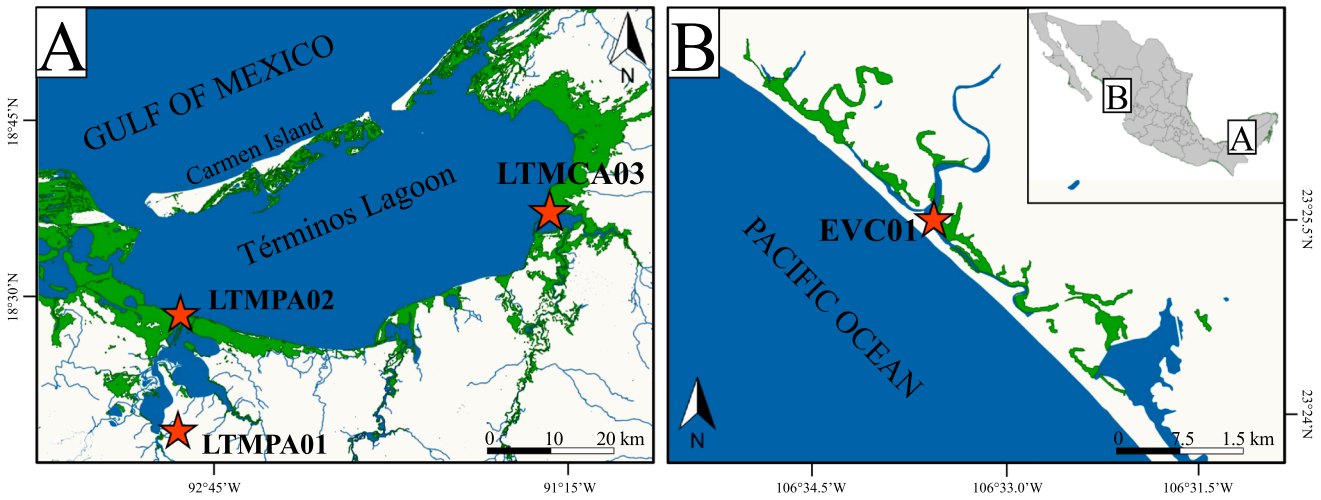

Fig. 1. Location of the sediment cores (★) from (A) Términos Lagoon (southern Gulf of Mexico) and (B) El Verde Camacho Lagoon (entrance of the Gulf of California). Green shading indicate the presence of mangrove areas.

Lafargue et al., 1998) were calculated to assess the C_{org} concentration and stability. The pyrolyzed carbon (PC, in %) corresponds to the carbon species (HC, CO, and CO_2) released during the pyrolysis stage, whereas the residual carbon (RC, %) is the most refractory fraction released as CO and CO_2 during the oxidation phase. The total organic carbon (TOC, %) content is the sum of the PC and RC fractions. The hydrogen index (HI, mg HC g^{-1} TOC) represents the quantity of HC produced during pyrolysis normalized to the TOC, indicating the hydrogen richness of OM, whereas the oxygen index (OI, mg CO_2 g^{-1} TOC) is the amount of oxygen released as CO and CO_2 during the pyrolysis and oxidation phases normalized to the TOC, indicating the oxygen richness and/or oxidation degree of OM.

The parameter R400 (i.e., the fraction of the S2 pyrogram integrated before 400 °C) was used to qualitatively interpret the diagenetic evolution of labile *versus* refractory C_{org} (Disnar et al., 2003). This is based on the concept that pyrolysis for readily labile biological compounds is generally finished at 400 °C, R400 is typically expressed as a percentage of the total integrated S2 curve. A novel parameter, $R400_{PC}$ (mg HC g^{-1}), was defined in this study to facilitate the quantitative interpretation of R400. It was calculated by multiplying R400 (%) by the quantity of PC content in the S2 curve (mg HC g^{-1}).

Three core sections (top, intermediate, and bottom) were defined to investigate distinct depositional conditions and diagenetic processes influencing the C_{org} quantity and stability along the cores based on the variation in Rock-Eval parameters. The non-parametric Kruskal-Wallis one-way analysis of variance and post-hoc Dunn tests were used to evaluate the differences in the rank distribution of Rock-Eval parameter values among cores. Additionally, associations between variables were assessed using Spearman correlation analysis and Student's *t*-test. All analyses were conducted with a confidence level of 95 %.

3.2.2. Analysis of organic matter source and stability

A pseudo van Krevelen diagram (HI *versus* OI) was used to identify OM sources, stability, and diagenetic processes (Baudin et al., 2015). Higher HI and lower OI values indicate thermally labile organic material from lacustrine (Type I) or marine (Type II) phytoplankton sources. Conversely, lower HI and higher OI values (Type III) indicate terrestrial inputs or well-oxidized organic material from Types I and II (Le Meur et al., 2021). The S2 pyrogram often does not follow a Gaussian distribution in immature samples such as mangrove sediments. Instead, it has multiple peaks or shoulders, indicating that the samples consist of a mixture of different fractions or clusters of organic components undergoing thermal degradation at various specific temperatures (e.g., Disnar and Trichet, 1984; Disnar et al., 2003; Sebag et al., 2016). To identify these distinct clusters from the multilobed S2 signal, mathematical deconvolution was used to isolate five elemental Gaussian distributions with peaks at well-defined temperatures of 300 °C, 360 °C, 415 °C, 470 °C, and 560 °C (±15 °C) (Table S1; Figs S1 to S4 in Supplementary Material). A semi-quantitative calculation determined the relative contributions (%) of each organic component pool from the S2 signal (Disnar et al., 2003; Le Meur et al., 2021). This contribution was then multiplied by the PC content (mg HC g^{-1}) in the S2 curve and expressed as a ratio to sediment mass (mg HC g^{-1}).

3.3. Palynofacies analysis

Five to six samples (~1 g) of each sediment core were selected in sections with apparent changes, peaks, or transitions observed in the Rock-Eval parameters TOC, HI, and OI. These changes served as indicators of potential shifts in the C_{org} quantity and stability within the sediment. Carbonates and silicates were eliminated using hydrochloric (50 mL) and hydrofluoric (50 mL) acids (Graz et al., 2010). Remnants were examined with a transmitted light microscope or under UV excitation (ZEISS Axioscope 5 Polarisation coupled to a camera ZEISS Axiocam 305 color) using a 50x magnification objective (Fig. 2).

Morphological and textural criteria allowed us to identify four main categories of components: (1) amorphous organic matter (AOM), lacking any discernible biological structures; (2) algal organic matter (algOM) derived from phytoplankton production, identified under UV light owing to the fluorescence of hydrocarbon-rich fractions (Boussafir et al., 2012); (3) lignocellulosic (LC) particles originating from higher plants characterized by an elongated shape; and (4) other particles with distinct and easily recognizable morphology (e.g., pollen, membrane) (Table 1). According to their characteristics, the particles were categorized as (a) preserved, including preserved or slightly degraded LC, cuticular and mycelial fragments, membranes, spores, pollen grains, and algOM; or (b) degraded, including floccular and gelified AOM, gelified and opaque LC, and opaque detritus.

Mass concentration of the particles was determined using a known pollen standard (10 mg mL^{-1}) incorporated into the samples (Battarbee and Kneen, 1982; de Vernal et al., 1987). *Cupressus* sp. was chosen as the standard because its strong reaction under UV excitation precludes confusion. Study particles and standards were counted per area unit delimited by the microscope's field of view. To ensure variations in relative abundances remained below 5 %, at least 500 area units per sediment sample were counted (Di-Giovanni et al., 1998; Sebag et al., 2006; Graz et al., 2010). The mass concentration of particles (mg g^{-1}) was estimated using the ratio between the areas (%) of studied particles

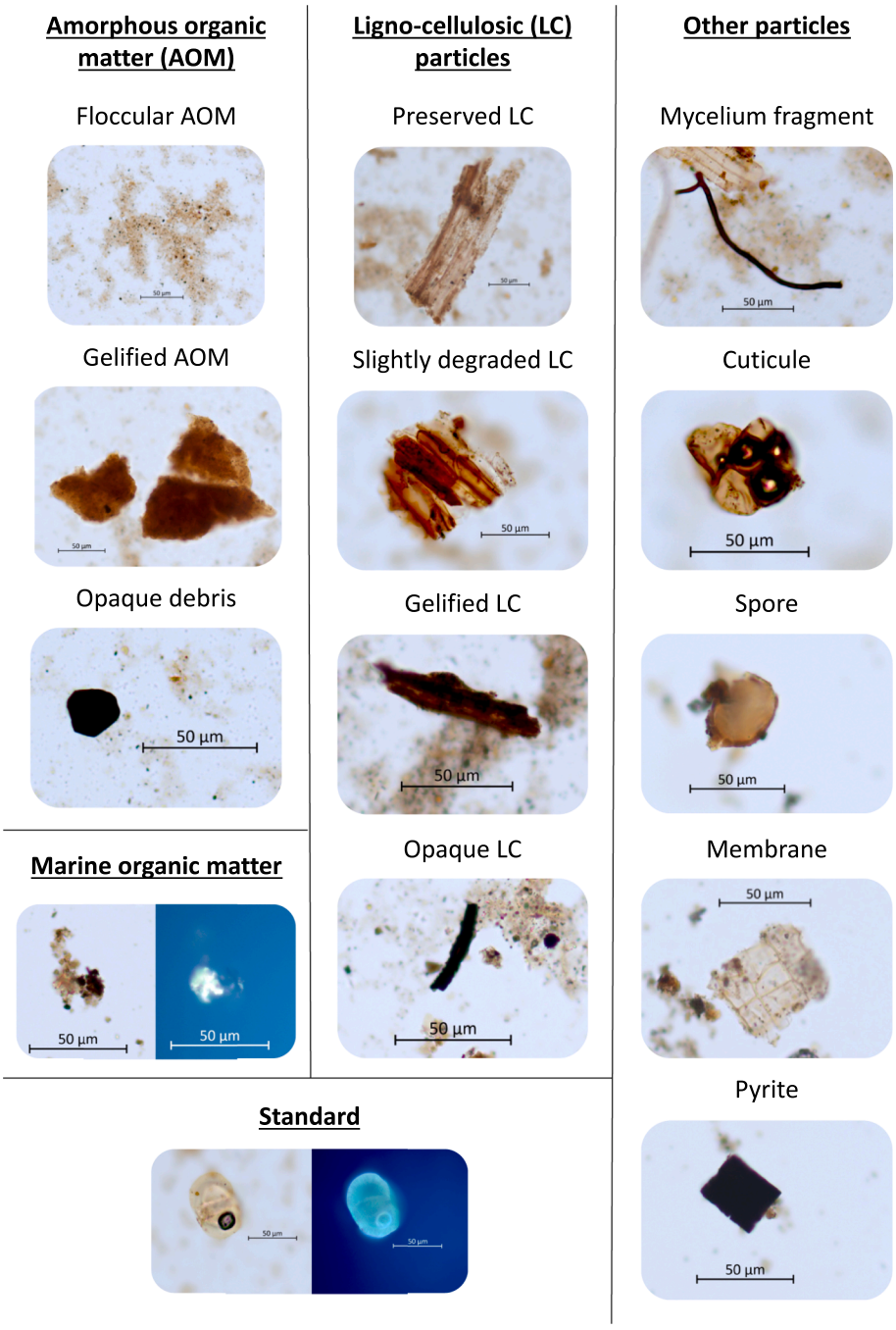

Fig. 2. Palynofacies categories in mangrove sediment cores from Términos Lagoon (southern Gulf of Mexico) and El Verde Camacho Lagoon (entrance of the Gulf of California).

and standards, multiplied by the standard mass concentration (mg mL^{-1}) in the sample (Graz et al., 2010).

3.4. Labile and refractory organic carbon stocks

The Rock-Eval-derived C_{org} stocks (i.e., the quantity of C_{org} stored per unit area, Mg ha^{-1}) were calculated per decade (C_{org} stocks$_{-10yr}$) and for the period from 1921 to 2021 (C_{org} stocks$_{-1921-2021}$) as the product of dry bulk density, section thickness, and C_{org} concentration (Howard et al., 2014). Labile C_{org} stocks included the most labile fraction of the PC (i.e., R400), whereas refractory C_{org} stocks were defined as the sum of the carbon pyrolyzed after 400 °C and the RC. The CO_2 equivalent (CO_{2eq}) emissions in case of significant loss of labile C_{org} fraction were calculated as the product of the labile C_{org} stocks, and the conversion factor of 3.67 (i.e., the ratio of C to CO_2 molecular weights) and were expressed as CO_{2eq} per hectare (Mg ha^{-1}) at decadal scale and over the 1921–2021 period (Howard et al., 2014).

4. Results

4.1. Basic Rock-Eval parameters

TOC in the sediment cores ranged from 0.38 % to 8.81 %, with a median of 2.17 % (Table 2). RC constituted the major fraction of the TOC (71–80 %), with PC at 20–29 %. The HI values ranged from 93 to 354 mg HC g^{-1} TOC, and OI values ranged from 115 to 332 mg CO_2 g^{-1} TOC,

Table 1
Characteristics of the organic particles in mangrove sediment cores form Términos Lagoon (southern Gulf of Mexico) and El Verde Camacho Lagoon (entrance of the Gulf of California).

Class	Abbreviation	Category	Characteristics	Group of preservation state
Amorphous particles	fAOM	Floccular amorphous organic matter	Diffuse edges. Gray to yellow in transmitted light, and opaque or slightly orange in reflected light. Size 10–100 μm.	Degraded
	gAOM	Gelified amorphous organic matter	Entirely gelified, without internal structure. Orange to red in transmitted light and dark orange in reflected light. Size can exceed 100 μm.	Degraded
	OD	Opaque debris	Sharp contours, high reflectance, and appears dark in transmitted light. Size ~ 10 μm.	Degraded
Phytoplankton particles	algOM	Algal OM	Transparent in reflected light. Brilliant yellow particles under fluorescent light.	Preserved
Lignocellulosic particles	PLC	Preserved or slightly degraded lignocellulosic	Elongated particles with visible internal structures, yellow in transmitted light. Size 10–100 μm.	Preserved
	GLC	Gelified lignocellulosic	Elongated particles with visible internal structures, yellow to orange in transmitted light. Size from 10 μm, and up to 100 μm with increased gelification.	Degraded
	OCL	Opaque lignocellulosic	No visible internal structure. Elongated. High reflectance. Size 10–100 μm.	Degraded
Other organic particles	Div	Preserved diverse organic particle	Mycelium fragments elongate, brown.	Preserved
			Cuticular fragments brown and with edges and botanic structures. Size variable and can exceed several hundred μm.	Preserved
			Spores and pollen grains from terrestrial and aquatic flora. Translucent or yellow when fresh, brown-orange when preserved.	Preserved
	Pyr	Pyrite	Opaque with geometrical forms under transmitted light	Degraded

Table 2
Rock-Eval parameters and clusters of organic components (C1 to C5) in mangrove sediment cores from Términos Lagoon (southern Gulf of Mexico) and El Verde Camacho Lagoon (entrance of the Gulf of California).

Variable	Statistics	LTMPA01	LTMPA02	LTMCA03	EVC01
TOC	Min	1.66	0.97	2.19	0.38
(%)	Max	8.14	3.25	8.81	3.91
	Mean	3.02	1.63	3.96	1.27
PC	Min	0.32	0.23	0.54	0.10
(%)	Max	2.18	0.95	3.17	0.87
	Mean	0.68	0.42	1.14	0.25
RC	Min	1.34	0.74	1.65	0.28
(%)	Max	5.96	2.30	5.64	3.04
	Mean	2.34	1.20	2.81	1.01
HI	Min	129	131	204	93
(mg HC g^{-1}	Max	218	251	354	195
TOC)	Mean	162	179	255	130
OI	Min	137	191	115	179
(mg CO_2 g^{-1}	Max	208	332	198	237
TOC)	Mean	182	255	154	211
R400	Min	0.36	0.30	0.27	0.23
(%)	Max	0.45	0.44	0.35	0.44
	Mean	0.40	0.36	0.29	0.34
$R400_{PC}$*	Min	3.54	2.40	2.96	1.84
(mg HC g^{-1} sed.)	Max	7.81	4.04	5.25	3.75
	Mean	4.40	3.12	3.78	2.67
C1*	Min	1.22	1.30	0.09	0.72
(mg HC g^{-1} sed.)	Max	3.41	4.43	1.23	3.03
	Mean	2.14	2.80	0.66	1.79
C2*	Min	0.64	1.68	3.38	2.04
(mg HC g^{-1} sed.)	Max	3.78	6.55	6.82	5.94
	Mean	2.38	2.93	4.87	3.92
C3*	Min	3.53	0.36	1.21	2.23
(mg HC g^{-1} sed.)	Max	8.75	4.61	3.58	5.51
	Mean	5.09	3.41	2.72	3.33
C4*	Min	5.22	6.23	7.18	6.16
(mg HC g^{-1} sed.)	Max	8.59	8.69	9.88	10.87
	Mean	7.08	7.47	8.84	7.95
C5*	Min	0.22	0.60	0.19	0.00
(mg HC g^{-1} sed.)	Max	1.36	1.28	0.80	0.96
	Mean	0.89	0.98	0.49	0.58

TOC, total organic carbon; PC, pyrolyzed carbon; RC, residual carbon; HI, hydrogen index; OI, oxygen index; R400 and $R400_{PC}$, hydrocarbons produced during pyrolysis before 400 °C with respect to the PC; C1-C5, clusters of organic components.

* Calculated as a ratio to sediment mass (see Methods).

indicating a general prevalence of terrestrial type (III) OM in the Van Krevelen pseudo-diagram (Fig. 3) across sediment cores. However, TOC, PC and HI values were significantly higher in LTMCA03 compared to other cores (LTMCA03 > LTMPA01 > LTMPA02 > EVC01), suggesting a higher proportion or better preservation of algal or mangrove-derived OM in this specific core. The OI values were significantly higher in LTMPA02 (>250 mg CO_2 g^{-1} TOC) than in the other cores (LTMPA02 > EVC01 > LTMPA01 > LTMCA03). R400 accounted for 29 % to 40 % of the S2 peak, and $R400_{PC}$ ranged from 1.84 to 7.81 mg HC g^{-1}.

The parameters TOC, PC, and RC exhibited strong correlations across all cores ($0.92 \leq r \leq 0.99$; $p < 0.05$). With increasing depth, TOC, PC, and RC values generally decreased in the top sections, showed low variability in intermediate sections, and increased by 1.12–1.24 % in LTMPA01 and LTMCA03, or remained unchanged in LTMPA02 and EVC01 in the bottom sections (Fig. 4). However, at 28–36 cm in LTMPA02 and 49–67 cm in LTMCA03, TOC, PC, and RC tended to increase with depth. In each core, TOC, R400, and $R400_{PC}$ increased from the 1950s to the 1960s, then accelerated towards the end of the century (Fig. 5).

HI and OI were significantly negatively correlated throughout the depth profile of LTMPA02 ($r = -0.75$, $p < 0.05$); no significant correlation was observed in the other cores. In the top sections of cores LTMPA02 and LTMCA03, trends of decreasing HI and increasing OI with depth were observed (Fig. 4). Contrasting changes in HI and OI were noted in the bottom sections of all cores. During the dating period, cores LTMPA01, LTMPA02, and LTMCA03 had a significant correlation between TOC and HI ($0.75 \leq r \leq 0.98$; $p < 0.05$), with both parameters showing increasing trends over time (Fig. 5). TOC and OI were negatively correlated in LTMPA02 ($r = -0.75$, $p < 0.05$) and positively correlated in LTMPA01 and EVC01 ($0.70 \leq r \leq 0.84$; $p < 0.05$).

4.2. Clusters of organic components

The dominant cluster was C4 (470 ± 15 °C), constituting 42–51 % of the total S2 peak, with concentrations ranging from 5.22 to 10.87 mg HC g^{-1} sed. (Table 1). On average, the second dominant clusters were C2 (360 ± 15 °C) in LTMCA03 (29 %) and EVC01 (25 %), and C3 (415 ± 15 °C) in the PDE system cores (LTMPA01: 27 %; LTMPA02: 19 %). C1 at 300 ± 15 °C (4–14 %) and C5 at 560 ± 15 °C (3–5 %) were minor clusters.

Generally, there was a trend of increasing C1 and decreasing C2 over depth (Figs. 4 and 5). A significant negative correlation between C1 and

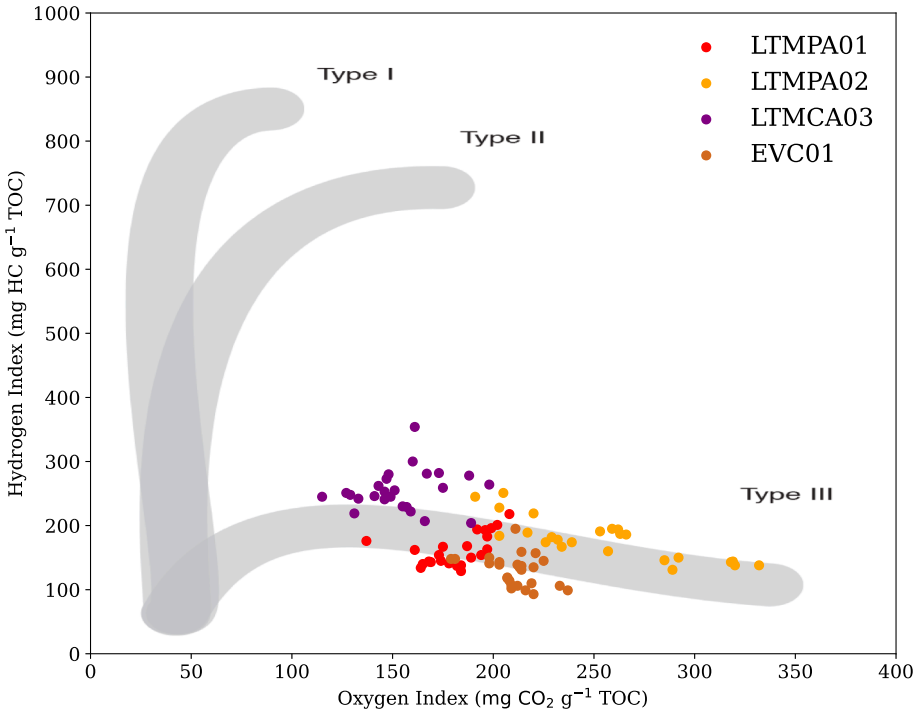

Fig. 3. Van Krevelen pseudo-diagram (Hydrogen Index *vs* Oxygen Index) for mangrove sediment cores from Términos Lagoon (southern Gulf of Mexico: LTM cores) and El Verde Camacho Lagoon (entrance of the Gulf of California: EVC core). TOC, total organic carbon; HC, hydrocarbons. Type of organic carbon: I, lacustrine; II, marine; III, terrestrial.

C2 was observed throughout all core depths of LTMCA03 ($r = -0.90$, $p < 0.05$). When considering only the dating period from 1918 to 2021, a significant negative correlation between C1 and C2 was also observed in LTMPA02 ($r = -0.79$, $p < 0.05$). C1 and C2 were not significantly correlated in cores LTMPA02 and EVC01. Clusters C3 and C4 showed little variations in the top and intermediate sections and were inversely related to each other in the bottom sections of the cores. No notable change was observed for cluster C5.

In sections 31–32 cm of LTMPA02, the S2 peak was unusual, showing two dominant peaks (Fig. S2 in Supplementary Material). As a consequence, these peaks, designated C2′ and C3′, were pyrolyzed at higher temperatures than the other depth sections, i.e., C2′ at 380 °C instead of the usual 360 °C for C2; C3′ at 430 °C instead of the usual 415 °C for C3.

4.3. Palynofacies identification

AOM was predominant among the palynofacies groups, comprising 70 % to 94 % of the total organic components in the cores (Fig. 6). Within this category, floccular AOM accounted for 49–92 %, whereas gelified AOM accounted for 1–38 %. LC particles accounted for only 5.6 % of the organic components among the cores, mostly in a gelified form (2.4 %). Preserved terrestrial organic particles (cuticular and mycelial fragments, membranes, spores, and pollen grains) constituted less than 1 % of all particles. The algOM accounted for 0.25 % in LTMPA01 and 1.02 % in the PDE cores but reached 3.80 % and 3.73 % in the top sections of cores LTMCA03 and EVC01. Degraded particles were dominant, constituting on average 92 % of the total particles in the samples from all cores (Fig. 6). Preserved particles were mainly concentrated in the top sections, with specific exceptions at 30–31 cm in LTMPA01, 31–32 cm in LTMPA02, and 47–48 cm in EVC01.

4.4. Organic carbon stocks

In the sediment cores, C_{org} stocks$_{\text{-}10yr}$ varied from 1.06–3.02 Mg ha^{-1} for 1921–1931 and 14.68–30.66 Mg ha^{-1} for 2011–2021. C_{org} stocks$_{\text{-}10yr}$ were highest (2.02–30.66 Mg ha^{-1}) in LTMPA01 and lowest (1.06–14.67 Mg ha^{-1}) in LTMPA02. The C_{org} stocks$_{\text{-}1921\text{-}2021}$ reached 42–89 Mg ha^{-1} among cores. Across all cores, C_{org} stocks$_{\text{-}10yr}$ increased from the early 1900 s to 2021, with noticeable acceleration after the 1950s (Fig. 7).

Throughout the period studied, the labile fraction represented 6–11 % of the total C_{org} stocks$_{\text{-}10yr}$, whereas refractory C_{org} stocks reached up to 89–94 % (Fig. 7). These proportions remained relatively constant over the last century, with a maximum difference of 0.3–2.1 % across all cores. The CO_{2eq} emissions that could be expected from the decomposition of the labile C_{org} stocks$_{\text{-}10yr}$ ranged from 0.35 to 12.10 Mg ha^{-1} across all cores, whereas those from the decomposition of the labile C_{org} stocks$_{\text{-}1921\text{-}2021}$ ranged from 13.8 to 31.2 Mg ha^{-1}.

5. Discussion

5.1. Sources and composition of organic matter

In all sediment cores, the restriction of OM to Type III on the Van Krevelen pseudo-diagram indicated that it was poor in hydrogenated compounds (hydrocarbons-rich OM) and rich in oxygenated ones (lignocellulosic-rich OM) (Fig. 3). The values of HI (93–354 mg HC g^{-1} TOC) and OI (115–332 mg CO_2 g^{-1} TOC) indicated a high proportion of terrestrial detritus compared to other sources (e.g., mangrove- or marine-derived OM); land-derived debris is usually lignocellulosic with low HI values (<250 mg HC g^{-1} TOC) associated with high OI values (>100 mg CO_2 g^{-1} TOC) (Meyers and Lallier-Vergès, 1999). Results suggested minor contribution of fresh mangrove detritus (420–556 mg HC g^{-1} TOC in mangrove leaf; 323–480 mg HC g^{-1} TOC in mangrove wood; Marchand et al., 2008), and marine-derived OM (HI>400 mg HC g^{-1} TOC; OI<100 mg CO_2 g^{-1} TOC; Meyers and Lallier-Vergès, 1999) that typically comprise hydrogen-rich compounds. However, low HI and high OI values may also suggest the oxidation of OM from mangrove or marine sources, as oxidation typically results in a decrease in HI, a slight increase in OI, and a modification of OM stability (Meyers and Lallier-

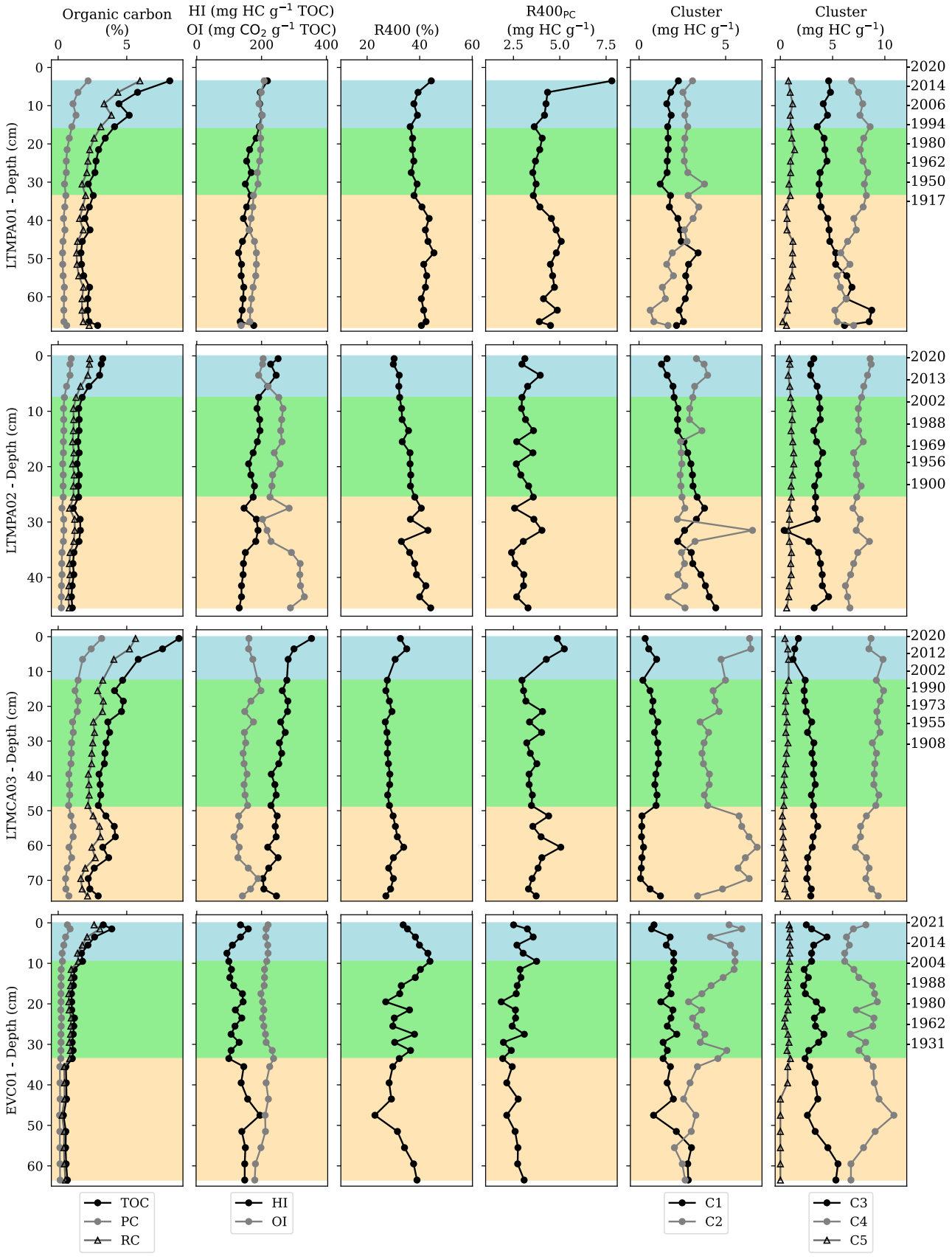

Fig. 4. Rock-Eval parameters (TOC, HI, OI, R400, and $R400_{PC}$) and clusters of organic components (C1 to C5) in mangrove sediment cores from Términos Lagoon (southern Gulf of Mexico) and El Verde Camacho Lagoon (entrance of the Gulf of California). Core sections: blue, bottom; green, intermediate; and yellow, bottom.

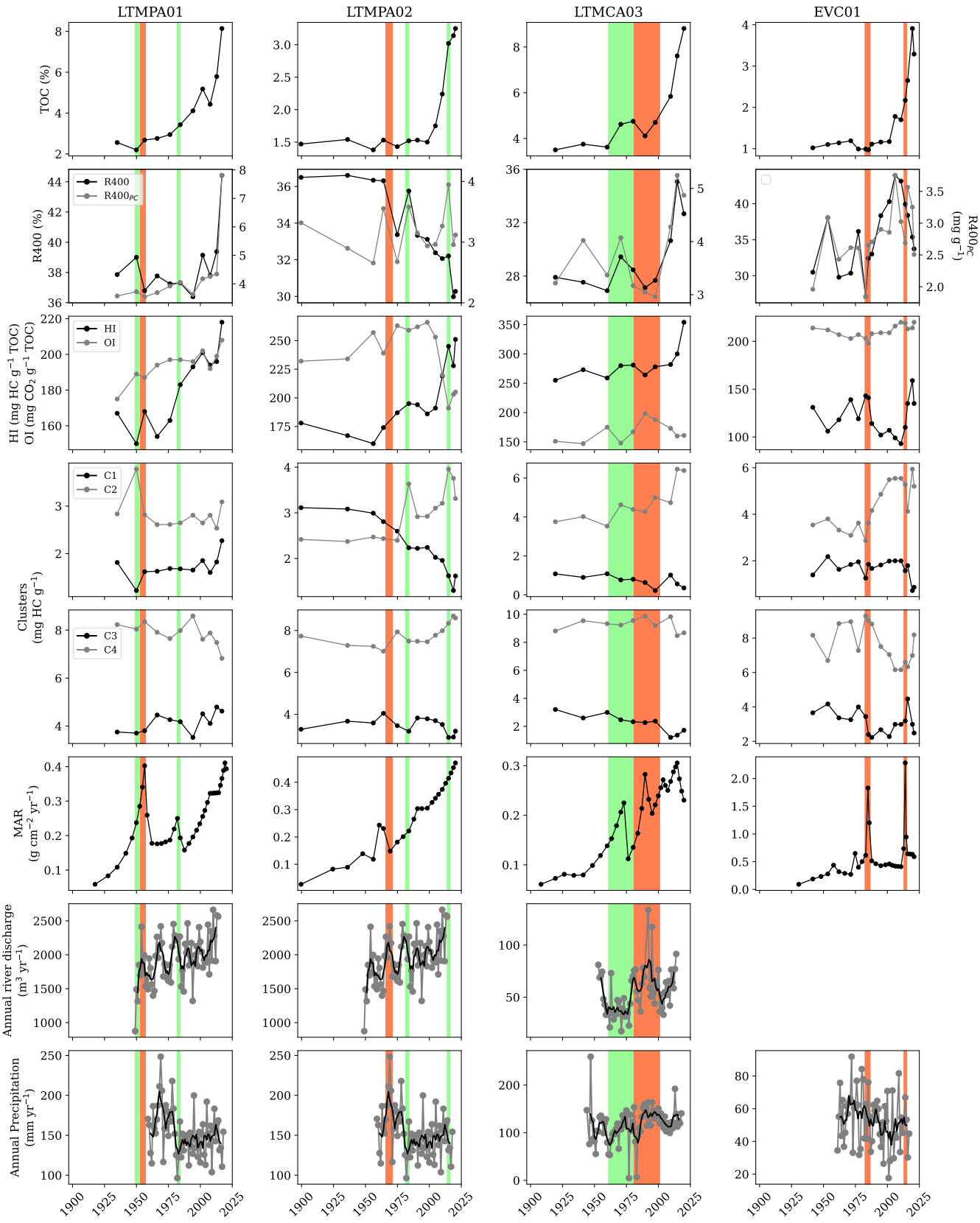

Fig. 5. Temporal variation of Rock-Eval parameters (TOC, HI, OI, R400, and R400$_{PC}$) and clusters of organic components (C1 to C5) in mangrove sediment cores from Términos Lagoon (southern Gulf of Mexico) and El Verde Camacho Lagoon (entrance of the Gulf of California). Time sections: green, events of enhanced organic carbon liability; red, events of decreased organic carbon liability. For mass accumulation rates (MAR), river discharges (when available), and precipitation data see Supplementary Material.

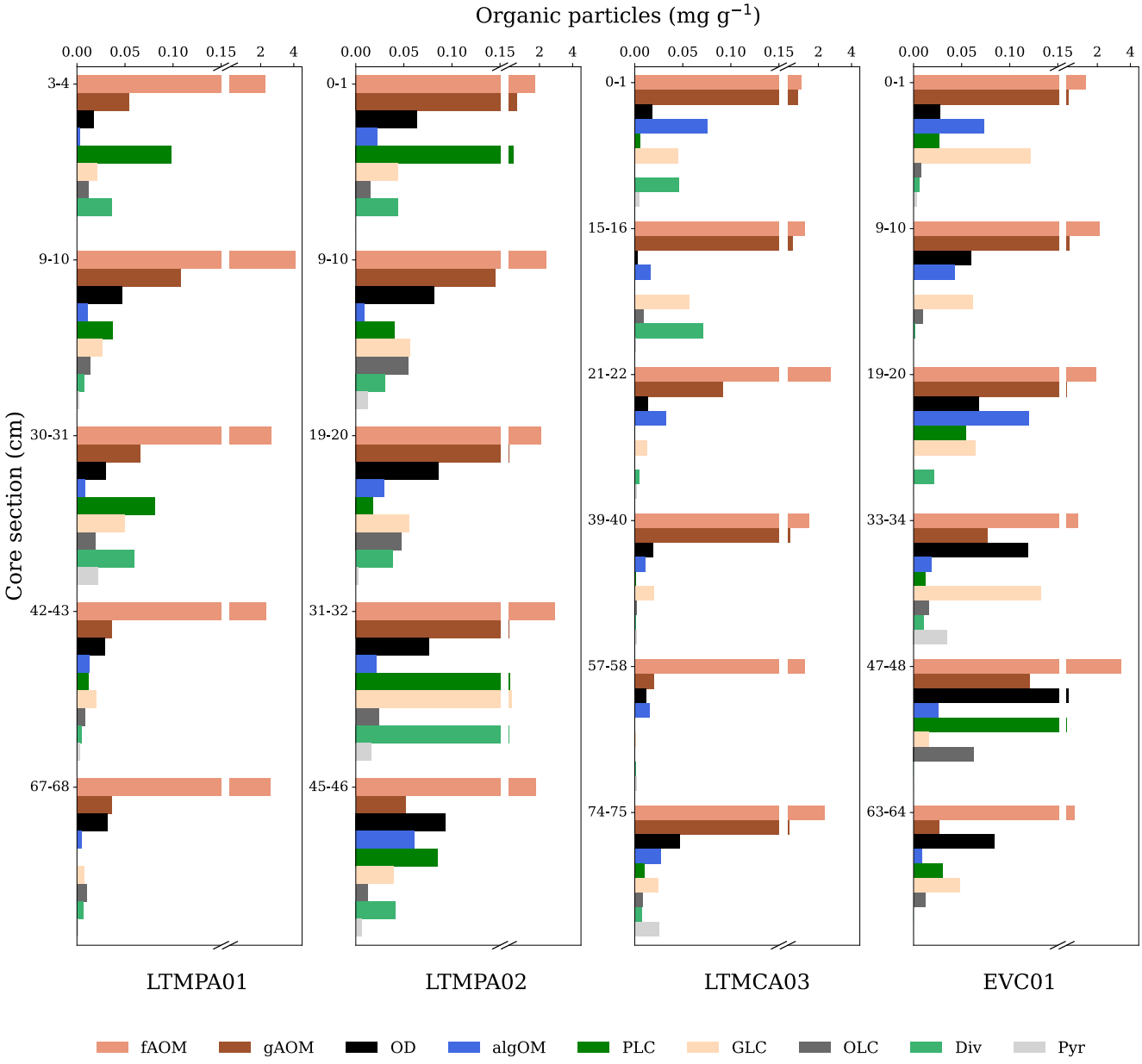

Fig. 6. Concentration of palynofacies in mangrove sediment cores from Términos Lagoon (southern Gulf of Mexico) and El Verde Camacho Lagoon (entrance of the Gulf of California). For palynofacies abbreviations see Table 1.

Vergès, 1999).

Although the Van Krevelen pseudo-diagram interpretation can provide insights into both the OM origin and liability, it may not directly pinpoint the specific contributions of each process (i.e., source and diagenetic state). However, the predominance of the palynofacies group AOM and the cluster C4 throughout the cores confirmed that most OM was in a refractory state when deposited in mangrove sediments. The AOM group indicated the presence of a mixture of plant, bacterial, algal, and planktonic fragments that have already undergone degradation (Batten and Stead, 2006; Sebag et al., 2006). The thermal breakdown of this mixture, observed at 470 ± 15 °C (C4), indicated high thermal stability and suggested resistance to microbial-driven decomposition. Low proportions of gelified AOM and LC suggested anoxic conditions during sequestration (Boussafir et al., 2012). Gelified LC typically originates from vascular plant tissues, likely mangrove leaves or wood, during the early stage of diagenesis under anoxic conditions (Lallier-Vergès et al., 1998).

The median C_{org} value of 2.17 % in these sites aligned with the global median of 2.2 % for mangrove ecosystems (Kristensen et al., 2008a). Consistent clusters of organic components and palynofacies across the cores indicated similarities in OM composition and sources among the mangrove sites. However, spatial variations in C_{org} concentrations were attributed to geomorphological, sedimentary, and local hydrological conditions specific to each site or core surroundings, influencing OM influx and preservation (Jupin et al., 2024b). The algal OM is more prone to decomposition than OM from higher plants and mangrove debris (Patience, 1996; Marchand et al., 2003; Ranjan et al., 2011), which may explain its relatively infrequent presence in the sediment cores. AlgOM contribution was higher in cores LTMCA03 and EVC01 from the smaller river systems (CP and EV), whereas the presence of algOM was less obvious in cores LTMPA02 and LTMPA01 from the PDE system, where the Palizada River dominates freshwater inputs to the Términos Lagoon (Contreras-Ruiz-Esparza et al., 2014).

Core LTMCA03 predominantly exhibited terrestrial characteristics with minor contribution of other OM sources, similar to cores LTMPA01, LTMPA02, and EVC01 (Fig. 3). However, significant higher values of

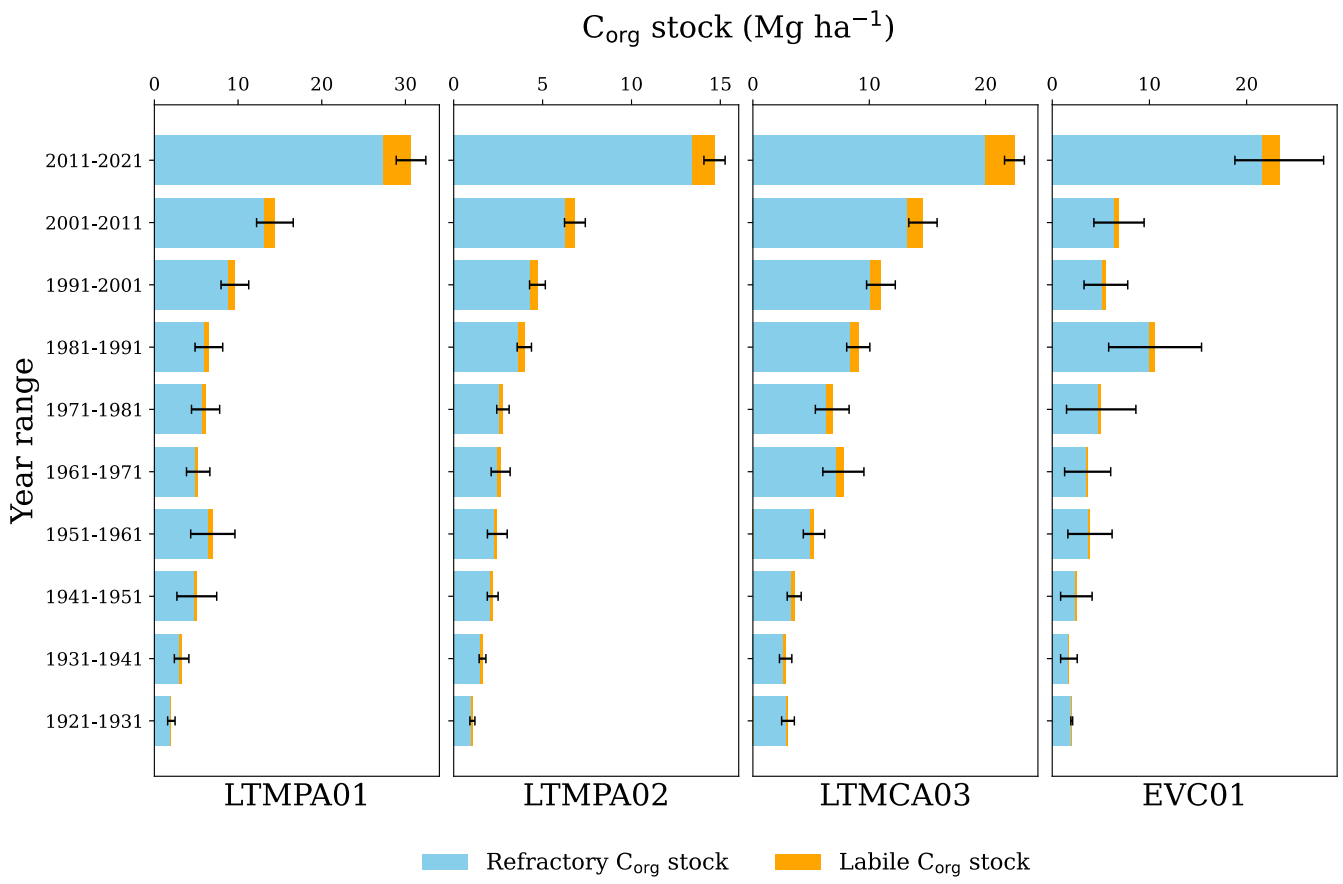

Fig. 7. Organic carbon stocks over 100 years in mangrove sediment cores from Términos Lagoon (southern Gulf of Mexico) and El Verde Camacho Lagoon (entrance of the Gulf of California).

TOC, PC, and HI, and lower values of OI in LTMCA03 suggested a greater influx of hydrogen-rich and labile or better-preserved OM in the CP system compared to other sites. Carbonate mangroves, such as those in the CP system, typically receive more autochthonous and labile OM inputs compared to terrigenous mangroves, such as the PDE and EV systems. This difference arises because carbonate mangroves have minimal allochthonous inputs of OM and sediments, minimizing dilution of deposited autochthonous OM (Jennerjahn, 2020; Twilley et al., 2018). The higher autochthonous OM contribution in LTMCA03 was supported by the highest concentrations of C2, associated with LC compounds (Disnar et al., 2003), such as mangrove tree wood and roots (Marchand et al., 2008). A better preservation of labile OM at this site could also be attributed to anoxic depositional conditions that inhibit microbial decomposition (Meyers, 1994). Evidence of recurrent anoxic conditions is supported by the higher proportion of gelified particles in LTMCA03 compared to other cores. These anoxic conditions may result from karstic water inputs characteristics of the CP system. Karstic waters typically exhibit temporary sub-anoxic to anoxic conditions (Bao et al., 2023) and were reported during the dry season in the CP system (Martínez-Trejo et al., 2024).

The high OI values in LTMPA02, particularly in sections from 25 to 26 cm and from 35 cm to the core bottom, indicated a high degree of oxidation or degradation of the OM (Boussafir et al., 2012) during specific periods. The presence of amorphized and gelified LC particles, along with high concentrations of C5 and opaque LC particles, aligned with prolonged oxidation phases (Boussafir et al., 2012). These periods may correspond to variations in the dynamics of the Palizada River, which influences the LTMPA02 area, as river discharge can promote sedimentary OM's resuspension, export, and aerobic decomposition (Kusumaningtyas et al., 2019; Allais et al., 2024). In contrast, LTMPA01, collected from an upstream mangrove creek within the PDE system, experienced higher autochthonous OM inputs and lability than LTMPA02, due to the lack of direct influence from the Palizada River.

5.2. *Temporal variability in quantity and liability of sedimentary organic carbon*

In the top sections of the cores LTMPA02 (2000–2021) and LTMCA03 (1990–2021), the decrease in HI values with depth indicated the dehydrogenation of organic compounds and the loss of hydrogen bonds, whereas the increase in OI values with depth was associated with mineralization and carbon loss, reflecting an oxidation profile (Meyers, 1997). This progressive shift was associated with a decline in TOC and $R400_{PC}$, indicating reduced C_{org} quantity and lability with increasing depth. Additionally, decreasing C2 values and increasing C1 values with depth were attributed to the progressive degradation of C2 organic components into smaller C1 compounds (Disnar et al., 2003). The gradual decrease in well-preserved particles, particularly LC, in the top sections coincided with the decline in C2 associated with mangrove detritus.

In the top section of core EVC01, decreasing HI values and stable OI values with depth may indicated an initial stage of decomposition of higher plant debris, mainly affecting the easily degradable hydrogen bounds (Marchand et al., 2003); however, the isolated peak in $R400_{PC}$ and C3 in 2014 ± 3 suggested a recent C_{org} supply. In the top section of LTMPA01, increasing values of HI, OI, and labile clusters (C1 and C2) towards the surface, associated with increasing values of TOC, PC, RC, and $R400_{PC}$, indicated a recent increase in labile C_{org} inputs to sediments. The increase in C_{org} quantity and lability in recent times in cores EVC01 and LTMPA01 may also be attributed to enhanced C_{org}

preservation owing to increased sediment accumulation rates (Jupin et al., 2023). Higher sediment deposition accelerates C_{org} burial, reducing exposure to aerobic conditions and promoting preservation (Burdige, 2007; Morris et al., 2016; Cuellar-Martinez et al., 2020).

River discharge, influenced by precipitation, regulates sediment, C_{org}, and nutrient transport in the TL and EV basins. Increased river discharge can promote sediment resuspension and C_{org} aerobic decomposition, preventing long-term C_{org} accumulation (Kusumaningtyas et al., 2019). In these cores, decreasing values of TOC, $R400_{PC}$, HI, and C2, alongside increasing OI and C4 values, were associated with high river discharge and precipitation (Fig. 5), such as in 1964 ± 4 in LTMPA02 and 1980–2000 in LTMCA03, indicating increased fluvial refractory C_{org} inputs to mangrove sediments. On the contrary, rising values of TOC, HI, $R400_{PC}$, and contributions of C2 and well-preserved particles, along with reduced OI and C3 values, indicated enhanced C_{org} quantity and lability in LTMPA01 at 31–32 cm (1947 ± 7), in LTMPA02 at 3–4 cm (2015.0 ± 0.6), at 13–14 cm (1984 ± 3) and 31–32 cm (>100 yr), in LTMCA03 at 18–25 cm (1961–1981), and in EVC01 at 19–21 cm (1977–1983). When data on river discharge and precipitation were available for comparison with the palynofacies data, such as in 1947 ± 7 for LTMPA01 and in 1976 ± 3 for LTMCA03, the increasing C_{org} quantity and lability were associated with a substantial proportion of preserved LC and other preserved organic particles (mycelial and cuticular fragments, spores, and pollen grains), and low river discharge and precipitation. This indicated that reduced riparian influence allowed a more significant contribution of autochthonous and well-preserved mangrove detritus to the total C_{org} accumulated.

The presence of two dominant peaks in the S2 spectrum at 31–32 cm in LMPA02 indicated two OM types with distinct preservation states during similar periods. Palynofacies analysis revealed a predominance of degraded particles (floccular AOM, gelified AOM, opaque debris, and gelified LC) in that core, along with high proportions of preserved LC and cuticular fragments derived from vascular plants compared to the proportions in the bottom sections of other cores. This suggests a reduction in Palizada River influence more than 100 years ago, although no river discharge data confirm this. In EVC01, MAR peaks in 1985 ± 9 and 2014 ± 3, previously linked to hurricanes (Jupin et al., 2023), were associated with increased TOC, $R400_{PC}$, HI, and C3, likely resulting from high-energy events facilitating material trapping by mangrove roots and higher C_{org} deposition (Smoak et al., 2013). Palynofacies data indicate increased preserved LC and algOM in 1985 ± 9, suggesting rapid accumulation and preservation of mangrove and marine-derived C_{org}. As the Gulf of California experienced higher rainfall and major hurricanes during El Niño conditions (Farfán *et al.*, 2013), this event was possibly related to the intense El Niño event of 1982–1983 and hurricane Tico on 11–24 October 1983 (Gunther and Cross, 1984). The MAR peak in 2014 ± 3, with similar variations in Rock-Eval parameters, may relate to the intense El Niño event of 2014–2016.

5.3. Are the studied mangroves a sink or source of atmospheric CO_2?

For C_{org} stocks to play a significant role in climate mitigation and blue carbon management, it is important to determine whether C_{org} stocks are prone to remineralization or stable over time (Howard et al., 2021). The relative proportions of labile and refractory material would be expected to change during the early stage of diagenesis because the degradation of OM by microbial activity is generally selective, with labile organic materials typically degrading more easily than refractory ones (Benner et al., 1990; Meyers, 1997; Southward et al., 2005). The most labile part of the pyrolyzed carbon (R400) is particularly susceptible to decomposition in the sediment column (Disnar et al., 2003), potentially leading to CO_2 emissions during the early diagenesis in mangrove sediments. In contrast, the refractory C_{org} stocks, such as woody material or organic compounds highly resistant to pyrolysis, require temperatures exceeding 400 °C for breakdown (Disnar et al., 2003). Although evidence of decomposition of recalcitrant organic components has been found in mangrove sediments, which depends on the stage of evolution of the mangrove forest and the redox conditions, low decomposition rates were reported under anoxic conditions (Marchand et al., 2003, 2005, 2008; Lallier-Vergès et al., 2008). The low proportion of highly labile C_{org} stocks and minimal change in the proportions between labile and refractory C_{org} stocks along the cores, including the top sections, confirmed that most C_{org} degradation occurred before burial and indicated limited potential for CO_{2eq} emissions from labile C_{org} decomposition. The predominance of refractory C_{org} stocks, as confirmed by palynofacies analysis, indicated the potential of these mangrove ecosystems as long-term C_{org} sinks.

The upward trends in C_{org} concentrations and $stocks_{\text{-}10yr}$ were partly due to increased river discharge since the 1950 s in the TL (Benítez et al., 2005; Soto-Galera et al., 2010; Fichez et al., 2017; no available data for EV), and the consequent increase in sediment inputs from rivers to these mangrove areas (Fig. 5; Jupin et al., 2023). Previous studies have shown that the increasing discharge from Usumacinta and Candelaria rivers was unrelated to precipitation (Benítez et al., 2005; Fichez et al., 2017); indeed, precipitation tended to decrease from 1959 to 2018 in the Usumacinta River Basin (Jupin et al., 2024a). The increasing sediment discharge by rivers has been attributed to exacerbated continental erosion caused by population growth and changes in land use and land cover (Benítez et al., 2005; Fichez et al., 2017; Jupin et al., 2023).

The observation of C_{org} decomposition, inferred from the relative proportions of labile and refractory C_{org} $stocks_{\text{-}10yr}$, may be underestimated, as decomposition in anoxic and saturated mangrove sediments is generally slow (Lallier-Vergès et al., 2008) compared to the recent and rapid accumulation of refractory C_{org} in these sites. Moreover, variations in Rock-Eval parameters showed sporadic changes in OM lability and nature, as a result of OM provenance changes, potentially complicating oxidation profiles and accurate assessments of C_{org} degradation rates. Despite C_{org} originating mainly from external sources and being refractory rather than newly formed from *in situ* capture of atmospheric CO_2, these mangroves have significantly contributed to accumulating allochthonous C_{org} in their sediments. Over time, mangroves have adapted to new sediment and C_{org} deposition patterns, resulting in greater C_{org} stocks. Typically, up to 90 % of total C_{org} stocks in mangrove ecosystems is stored in sediments (e.g., Phang et al., 2015; Ezcurra et al., 2016; Cooray et al., 2021). This may indicate that, overall, the C_{org} stocks in the studied mangroves can be considered stable and efficient C_{org} sinks over time; hence, the conservation of these ecosystems contributes significantly to mitigating climate change.

6. Conclusions

Rock-Eval pyrolysis and palynofacies analyses of mangrove sediment cores from two Mexican Ramsar sites showed similar provenance and composition of organic matter (OM) across the sampling sites, with specific differences among cores attributed to the influence of local sedimentary and hydrological conditions. Most of the observed sedimentary organic carbon (C_{org}) in this study was refractory and proceeds from terrestrial detritus. The high proportions of refractory C_{org} stocks and degraded organic particles in the cores indicated that the C_{org} degradation processes mainly occurred before its burial in the sediment column. A trend towards decreasing C_{org} concentration from 1990 to 2021 in some cores was attributed to early oxidative diagenesis of C_{org}, in agreement with decreasing hydrogen-rich and preserved compounds with depth. The increase in C_{org} concentrations and stocks over 1921–2021 was attributed to the increasing supply of refractory and riverine C_{org}, resulting from a century of deforestation and land-use change in the regions surrounding these mangroves, rather than the mangrove ecosystems themselves. However, mangroves efficiently served as long-term sinks for the external supply of refractory C_{org}. The Ramsar status of the studied ecosystems is appropriate in the face of the deleterious effects of global change; however, local mangrove conservation and management strategies should be improved to favor the

expansion and restoration of these ecosystems with high Blue Carbon sequestration potential.

CRediT authorship contribution statement

J.L.J. Jupin: Writing – original draft, Validation, Investigation, Formal analysis, Data curation. **M. Boussafir:** Writing – review & editing, Validation, Resources, Methodology, Investigation, Formal analysis. **A. Sifeddine:** Writing – review & editing, Supervision, Resources, Funding acquisition, Conceptualization. **A.C. Ruiz-Fernández:** Writing – review & editing, Validation, Supervision, Resources, Project administration, Methodology, Investigation, Funding acquisition, Formal analysis, Conceptualization. **J.A. Sanchez-Cabeza:** Writing – review & editing, Investigation, Conceptualization. **L.H. Pérez-Bernal:** Writing – review & editing, Methodology, Formal analysis, Data curation.

Declaration of competing interest

The authors declare that they have no known competing financial interests or personal relationships that could have appeared to influence the work reported in this paper.

Data availability

Data will be made available on request.

Acknowledgments

This study was developed with the support of Universidad Nacional Autónoma de México (UNAM) through the research grant IN102821 from PAPIIT-DGAPA and the mobility grants for JL Jupin from the Instituto de Ciencias del Mar y Limnología, the Centro de Estudios Mexicanos UNAM-Francia, and the Institut de Recherche pour le Développement (IRD) through the international network DEXICOTROP. J. L. Jupin acknowledges a Ph.D. fellowship provided by Consejo Nacional de Ciencia y Tecnología-Mexico (CONACYT, CVU 1102000) and expresses gratitude for the support received from the Posgrado en Ciencias del Mar y Limnologia, UNAM and the Laboratoire GéoHydrosystèmes COntinentaux from the Université de Tours. The authors thanks J. G. Cardoso-Mohedano., M. A. Gómez-Ponce, J. G. Flores-Trujillo, and J. A. Martinez-Trejo (sampling); L. F. Álvarez-Sánchez (data curation), C. Súarez-Gutiérrez (informatics); and A. Grant (English edition of the manuscript) for their valuable support. C. Le-Milbeau and R. Boscardin from the Institut des Sciences de la Terre d'Orléans, France, are acknowledged for their technical support in Rock-Eval analyses.

Appendix A. Supplementary data

Supplementary data to this article can be found online at https://doi.org/10.1016/j.catena.2024.108279.

References

Allais, L., Thibodeau, B., Khan, N.S., Crowe, S.A., Cannicci, S., Not, C., 2024. Salinity, mineralogy, porosity, and hydrodynamics as drivers of carbon burial in urban mangroves from a megacity. *Science of the Total Environment*. Elsevier b.v. 912, 168955 https://doi.org/10.1016/j.scitotenv.2023.168955.

Alongi, D.M., 2005. Mangrove-microbe-soil relations. In: Kristensen, E., Haese, R.R., Kostka, J.E. (Eds.), Interactions between Macro-and Microorganisms in Marine Sediments. American Geophysical Union, Washington, pp. 85–103.

Alongi, D.M., 2020. Global Significance of Mangrove Blue Carbon in Climate Change Mitigation (Version 1). *Sci.* MDPI AG 2 (3), 57. https://doi.org/10.3390/sci2030057.

Bach L, Calderon R, Cepeda MF, Oczkowski A, Olsen SB, Robadue D. 2005. *Resumen del Perfil de Primer Nivel del Sitio Laguna de Términos y su Cuenca, México. Coastal Resources Center, University of Rhode Island*. Coastal Resources Center, University of Rhode Island: Narragansett.

Bao, J., Wu, X., Zhang, Q., Yuan, D., Guo, F., Liu, F., 2023. Unveiling the nitrogen transport and transformation in different karst aquifers media. *Journal of Hydrology*. Elsevier b.v. 620 https://doi.org/10.1016/j.jhydrol.2023.129335.

Battarbee, R.W., Kneen, M.J., 1982. The use of electronically counted microspheres in absolute diatom analysis. Limnology and Oceanography 27 (1), 184–188. https://doi.org/10.4319/lo.1982.27.1.0184.

Batten, D.J., Stead, D.T., 2006. Palynofacies Analysis and its Stratigraphic Application. Applied Stratigraphy. Springer, Netherlands, pp. 203–226.

Baudin, F., Disnar, J.-R., Aboussou, A., Savignac, F., 2015. Guidelines for Rock-Eval analysis of recent marine sediments. *Organic Geochemistry*. Elsevier Ltd 86, 71–80. https://doi.org/10.1016/j.orggeochem.2015.06.009.

Benítez JA, Sanvicente Sánchez H, Lafragua Contreras J, Zamora Crescencio P, Morales Manilla LM, Mas Caussel JF, García Gil G, Couturier SA, Zetina Tapia R, Calan Yam RA, Amabilis Sánchez L, Acuña C, Mejenes M. 2005. Sistemas de información geográfica de la cuenca del río Candelaria: reconstrucción histórica de los cambios de cobertura forestal y su efecto sobre la hidrología y calidad del agua-marco teórico y resultados iniciales. In: Edith F and Kauffer M (eds) *El agua en la frontera México-Guatemala- Belice*. Ecosur/tnc/unach: Tuxtla Gutiérrez, Chiapas, 19–32.

Benner, R., Hatcher, P.G., Hedges, J.I., 1990. Early diagenesis of mangrove leaves in a tropical estuary: Bulk chemical characterization using solid-state 13C NMR and elemental analyses. Geochimica et Cosmochimica Acta 54 (7), 2003–2013. https://doi.org/10.1016/0016-7037(90)90268-P.

Borges, A.V., Djenidi, S., Lacroix, G., Théate, J., Delille, B., Frankignoulle, M., 2003. Atmospheric CO2 flux from mangrove surrounding waters. Geophysical Research Letters 30 (11), 12–15. https://doi.org/10.1029/2003GL017143.

Bouillon, S., Dahdouh-Guebas, F., Rao, A.V.V.S., Koedam, N., Dehairs, F., 2003. Sources of organic carbon in mangrove sediments: Variability and possible ecological implications. Hydrobiologia 495, 33–39. https://doi.org/10.1023/A:1025411506526.

Bouillon, S., Borges, A.V., Castañeda-Moya, E., Diele, K., Dittmar, T., Duke, N.C., Kristensen, E., Lee, S.Y., Marchand, C., Middelburg, J.J., Rivera-Monroy, V.H., Smith, T.J., Twilley, R.R., 2008. Mangrove production and carbon sinks: A revision of global budget estimates. Global Biogeochemical Cycles 22 (2), 1–12. https://doi.org/10.1029/2007GB003052.

Boussafir, M., Sifeddine, A., Jacob, J., Foudi, M., Cordeiro, R.C., Albuquerque, A.L.S., Abrao, J.J., Turcq, B., 2012. Petrographical and geochemical study of modern lacustrine sedimentary organic matter (Lagoa do Caçò, Maranão, Brazil): Relationship between early diagenesis, organic sedimentation and lacustrine filling. Organic Geochemistry 47, 88–98. https://doi.org/10.1016/j.orggeochem.2012.03.013.

Briseño-Dueñas, R., 2003. Ficha Informativa de los Humedales de Ramsar. (FIR). "Playa Tortuguera El Verde Camacho".

Burdige, D.J., 2007. The Controls on Organic Carbon Preservation in Marine Sediments. Geochemistry of Marine Sediments. Princeton University Press, Princeton, pp. 408–441.

Combaz, A., 1964. Les palynofaciès. Revue De Micropaléontologie 7 (3), 205–218.

Conagua, 2015. Determinación de la Disponibilidad de Agua en el acuífero Río Quelite (2508), estado de Sinaloa. Comisión Nacional Del Agua 25.

Contreras-Ruiz-Esparza, A., Douillet, P., Zavala-Hidalgo, J., 2014. Tidal dynamics of the Terminos Lagoon, Mexico: Observations and 3D numerical modelling. Ocean Dynamics 64 (9), 1349–1371. https://doi.org/10.1007/s10236-014-0752-3.

Cooray, P.L.I.G.M., Kodikara, A.S.K., Kumara, M.P., Jayasinghe, U.I., Madarasinghe, S.K., Dahdouh-Guebas, F., Gorman, D., Huxham, M., Jayatissa, L.P., 2021. Climate and intertidal zonation drive variability in the carbon stocks of Sri Lankan mangrove forests. *Geoderma*. Elsevier b.v. 389 https://doi.org/10.1016/j.geoderma.2021.114929.

Cuellar-Martinez, T., Ruiz-Fernández, A.C., Sanchez-Cabeza, J.A., Pérez-Bernal, L., López-Mendoza, P.G., Carnero-Bravo, V., Agraz-Hernández, C.M., van Tussenbroek, B.I., Sandoval-Gil, J., Cardoso-Mohedano, J.G., Vázquez-Molina, Y., Aldana-Gutiérrez, G., 2020. Temporal records of organic carbon stocks and burial rates in Mexican blue carbon coastal ecosystems throughout the Anthropocene. Global and Planetary Change, 192. Elsevier B.V, p. 103215. https://doi.org/10.1016/j.gloplacha.2020.103215.

de Vernal, A., Larouche, A., Richard, P.J.H., 1987. Evaluation of palynomorph concentrations: Do the aliquot and the marker-grain methods yield comparable results? Pollen et Spores XXIX(2–3), 291–304.

Díaz-Asencio, M., Sanchez-Cabeza, J.A., Ruiz-Fernández, A.C., Corcho-Alvarado, J.A., Pérez-Bernal, L.H., 2020. Calibration and use of well-type germanium detectors for low-level gamma-ray spectrometry of sediments using a semi-empirical method. Journal of Environmental Radioactivity 225 (June). https://doi.org/10.1016/j.jenvrad.2020.106385.

Di-Giovanni, C., Disnar, J.R., Bichet, V., Campy, M., Guillet, B., 1998. Geochemical characterization of soil organic matter and variability of a postglacial detrital organic supply (Chaillexon Lake, France). Earth Surface Processes and Landforms 23 (12), 1057–1069. https://doi.org/10.1002/(SICI)1096-9837(199812)23:12<1057::AID-ESP921>3.0.CO;2-H.

Disnar, J.R., 1994. Determination of maximum paleotemperatures of burial (MPTB) of sedimentary rocks from pyrolysis data on the associated organic matter: basic principles and practical application. Chemical Geology 118 (1–4), 289–299. https://doi.org/10.1016/0009-2541(94)90182-1.

Disnar, J.R., Guillet, B., Keravis, D., Di-Giovanni, C., Sebag, D., 2003. Soil organic matter (SOM) characterization by Rock-Eval pyrolysis: scope and limitations. Organic Geochemistry 34 (3), 327–343. https://doi.org/10.1016/S0146-6380(02)00239-5.

Disnar, J.-R., Trichet, J., 1984. The influence of various divalent cations (UO22+, Cu2+, Pb2+, Co2+, Ni2+, Zn2+, Mn2+) on the thermally induced evolution of organic

matter isolated from an algal mat. Organic Geochemistry 6, 865–874. https://doi.org/10.1016/0146-6380(84)90109-8.
Donato, D.C., Kauffman, J.B., Murdiyarso, D., Kurnianto, S., Stidham, M., Kanninen, M., 2011. Mangroves among the most carbon-rich forests in the tropics. *Nature Geoscience*. Nature Publishing Group 4 (5), 293–297. https://doi.org/10.1038/ngeo1123.
Duan, D., Lan, W., Chen, F., Lei, P., Zhang, H., Ma, J., Wei, Y., Pan, K., 2020. Neutral monosaccharides and their relationship to metal contamination in mangrove sediments. *Chemosphere*. Elsevier Ltd 251. https://doi.org/10.1016/j.chemosphere.2020.126368.
Espitalié, J., Laporte, J.L., Madec, M., Marquis, F., Leplat, P., Paulet, J., Boutefeu, A., 1977. Méthode rapide de caractérisation des roches mètres, de leur potentiel pétrolier et de leur degré d'évolution. Revue De L'institut Français Du Pétrole 32 (1), 23–42. https://doi.org/10.2516/ogst:1977002.
Espitalié, J., Deroo, G., Marquis, F., 1985a. La pyrolyse Rock-Eval et ses applications. Deuxième partie. *Revue de l'Institut français du Pétrole*. EDP. Sciences 40 (6), 755–784.
Espitalié, J., Deroo, G., Marquis, F., 1985b. Rock-Eval pyrolysis and its applications (part one). Oil & Gas Science and Technology-Revue d'IFPEN. EDP. Sciences 40 (5), 563–579.
Ezcurra, P., Ezcurra, E., Garcillán, P.P., Costa, M.T., Aburto-Oropeza, O., 2016. Coastal landforms and accumulation of mangrove peat increase carbon sequestration and storage. Proceedings of the National Academy of Sciences 113 (16), 4404–4409. https://doi.org/10.1073/pnas.1519774113.
Fichez, R., Archundia, D., Grenz, C., Douillet, P., Gutiérrez-Mendieta, F., Origel-Moreno, M., Denis, L., Contreras-Ruiz-Esparza, A., Zavala-Hidalgo, J., 2017. Global climate change and local watershed management as potential drivers of salinity variation in a tropical coastal lagoon (Laguna de Terminos, Mexico). *Aquatic Sciences*. Research across Boundaries, Springer Verlag 79 (2), 219–230. https://doi.org/10.1007/s00027-016-0492-1.
Flores-Verdugo FJ, Briseño-Dueñas R, González-Farías F, Calvario-Martínez O. 1995. Balance de carbono en un ecosistema lagunar estuarino de boca efímera de la costa noroccidental de México (Estero El Verde, Sinaloa). *Temas de oceanografía biológica en México. Universidad Autónoma de Baja California. Ensenada, 8.C., México.*, II.
Friess, D.A., Yando, E.S., Abuchahla, G.M.O., Adams, J.B., Cannicci, S., Canty, S.W.J., Cavanaugh, K.C., Connolly, R.M., Cormier, N., Dahdouh-Guebas, F., Diele, K., Feller, I.C., Fratini, S., Jennerjahn, T.C., Lee, S.Y., Ogurcak, D.E., Ouyang, X., Rogers, K., Rowntree, J.K., Sharma, S., Sloey, T.M., Wee, A.K.S., 2020. Mangroves give cause for conservation optimism, for now. *Current Biology*. Elsevier 30 (4), R153–R154. https://doi.org/10.1016/j.cub.2019.12.054.
García, E., 1973. Modificaciones al sistema de clasificación climática de Köppen: para adaptarlo a las condiciones de la república mexicana. Universidad Nacional Autónoma de México, México, D. F.
Graz, Y., Di-Giovanni, C., Copard, Y., Laggoun-Défarge, F., Boussafir, M., Lallier-Vergès, E., Baillif, P., Perdereau, L., Simonneau, A., 2010. Quantitative palynofacies analysis as a new tool to study transfers of fossil organic matter in recent terrestrial environments. International Journal of Coal Geology 84 (1), 49–62. https://doi.org/10.1016/j.coal.2010.08.006.
Gunther, E.B., Cross, R.L., 1984. Eastern North Pacific Tropical Cyclones of 1983. Monthly Weather Review 112, 1419–1440.
Holguin, G., Vazquez, P., Bashan, Y., 2001. The role of sediment microorganisms in the productivity, conservation, and rehabilitation of mangrove ecosystems: an overview. Biology and Fertility of Soils 33 (4), 265–278. https://doi.org/10.1007/s003740000319.
Howard J, Hoyt S, Isensee K, Telszewski M, Pidgeon E, (eds). 2014. *Coastal blue carbon: methods for assessing carbon stocks and emissions factors in mangroves, tidal salt marshes, and seagrasses*. Conservational International, Intergovernmental Oceanographic Commission of UNESCO, International Union for Conservation of Nature.: Arlington, Virginia, USA.
Howard JL, Lopes CC, Wilson SS, McGee-Absten V, Carrión CI, Fourqurean JW. 2021. Decomposition Rates of Surficial and Buried Organic Matter and the Lability of Soil Carbon Stocks Across a Large Tropical Seagrass Landscape. *Estuaries and Coasts*. Springer, 44(3): 846–866. Doi: 10.1007/s12237-020-00817-x.
Jennerjahn, T.C., 2020. Relevance and magnitude of "Blue Carbon" storage in mangrove sediments: Carbon accumulation rates vs. stocks, sources vs. sinks. *Estuarine, Coastal and Shelf Science*. Elsevier Ltd 247 (January), 107027. https://doi.org/10.1016/j.ecss.2020.107027.
Jupin, J.L.J., Ruiz-Fernández, A.C., Sifeddine, A., Sanchez-Cabeza, J.A., Pérez-Bernal, L. H., Cardoso-Mohedano, J.G., Gómez-Ponce, M.A., Flores-Trujillo, J.G., 2023. Anthropogenic drivers of increasing sediment accumulation in contrasting Mexican mangrove ecosystems. CATENA 226, 107037. https://doi.org/10.1016/j.catena.2023.107037.
Jupin, J.L.J., Garcia-López, A.A., Briceño-Zuluaga, F.J., Sifeddine, A., Ruiz-Fernández, A. C., Sanchez-Cabeza, J., Cardoso-Mohedano, J.G., 2024a. Precipitation homogenization and trends in the Usumacinta River Basin (Mexico-Guatemala) over the period 1959–2018. *International Journal of Climatology*. John Wiley and Sons Ltd 44 (1), 108–125. https://doi.org/10.1002/joc.8318.
Jupin, J.L.J., Ruiz-Fernández, A.C., Sifeddine, A., Mendez-Millan, M., Sanchez-Cabeza, J. A., Pérez-Bernal, L.H., Cardoso-Mohedano, J.G., Gómez-Ponce, M.A., Flores-Trujillo, J.G., 2024b. Terrestrial inputs boost organic carbon accumulation in Mexican mangroves. *Science of the Total Environment*. Elsevier b.v. 940 https://doi.org/10.1016/j.scitotenv.2024.173440.
Koné, Y.J.M., Borges, A.V., 2008. Dissolved inorganic carbon dynamics in the waters surrounding forested mangroves of the Ca Mau Province (Vietnam). Estuarine, Coastal and Shelf Science 77 (3), 409–421. https://doi.org/10.1016/j.ecss.2007.10.001.
Kristensen, E., Bouillon, S., Dittmar, T., Marchand, C., 2008a. Organic carbon dynamics in mangrove ecosystems: A review. Aquatic Botany 201–219.
Kristensen, E., Flindt, M.R., Ulomi, S., Borges, A.V., Abril, G., Bouillon, S., 2008b. Emission of CO2 and CH4 to the atmosphere by sediments and open waters in two Tanzanian mangrove forests. Marine Ecology Progress Series 370, 53–67. https://doi.org/10.3354/meps07642.
Kusumaningtyas, M.A., Hutahaean, A.A., Fischer, H.W., Pérez-Mayo, M., Ransby, D., Jennerjahn, T.C., 2019. Variability in the organic carbon stocks, sources, and accumulation rates of Indonesian mangrove ecosystems. *Estuarine, Coastal and Shelf Science*. Elsevier 218 (December 2018), 310–323. https://doi.org/10.1016/j.ecss.2018.12.007.
Lafargue, E., Marquis, F., Pillot, D., 1998. Rock-Eval 6 applications in hydrocarbon exploration, production, and soil contamination studies. Revue De L'institut Francais Du Petrole 53 (4), 421–437. https://doi.org/10.2516/ogst:1998036.
Lallier-Vergès, E., Perrussel, B.P., Disnar, J.R., Baltzer, F., 1998. Relationships between environmental conditions and the diagenetic evolution of organic matter derived from higher plants in a modern mangrove swamp system (Guadeloupe, French West Indies). Organic Geochemistry 29 (5–7–7 pt 2), 1663–1686. https://doi.org/10.1016/S0146-6380(98)00179-X.
Lallier-Vergès, E., Marchand, C., Disnar, J.R., Lottier, N., 2008. Origin and diagenesis of lignin and carbohydrates in mangrove sediments of Guadeloupe (French West Indies): Evidence for a two-step evolution of organic deposits. *Chemical Geology*. Elsevier b.v. 255 (3–4), 388–398. https://doi.org/10.1016/j.chemgeo.2008.07.009.
Le Meur, M., Boussafir, M., Le Milbeau, C., Debure, M., Claret, F., Robinet, J.-C., Lerouge, C., 2021. Organic matter oxidation of the Tégulines Clay formation, (Paris Basin, France): Spatial Heterogeneities. *Applied Geochemistry*. Elsevier Ltd 134, 105093. https://doi.org/10.1016/j.apgeochem.2021.105093.
Marchand, C., Lallier-Vergès, E., Baltzer, F., 2003. The composition of sedimentary organic matter in relation to the dynamic features of a mangrove-fringed coast in French Guiana. Estuarine, Coastal and Shelf Science 56 (1), 119–130. https://doi.org/10.1016/S0272-7714(02)00134-8.
Marchand, C., Disnar, J.R., Lallier-Vergès, E., Lottier, N., Lallier-Vergès, E., Lottier, N., 2005. Early diagenesis of carbohydrates and lignin in mangrove sediments subject to variable redox conditions (French Guiana). Geochimica et Cosmochimica Acta 69 (1), 131–142. https://doi.org/10.1016/j.gca.2004.06.016.
Marchand, C., Lallier-Vergès, E., Disnar, J.R., Kéravis, D., 2008. Organic carbon sources and transformations in mangrove sediments: A Rock-Eval pyrolysis approach. Organic Geochemistry 39 (4), 408–421. https://doi.org/10.1016/j.orggeochem.2008.01.018.
Martínez-Trejo JA, Cardoso-Mohedano JG, Sanchez-Cabeza JA, Ayón JMH, Ruiz-Fernández AC, Gómez-Ponce MA, Barranco L, Pech D. 2024. Variability of Dissolved Inorganic Carbon in the Most Extensive Karst Estuarine-Lagoon System of the Southern Gulf of Mexico. *Estuaries and Coasts*. Springer. Doi: 10.1007/s12237-024-01384-1.
Meyers, P.A., 1994. Preservation of elemental and isotopic source identification of sedimentary organic matter. Chemical Geology 114 (3–4), 289–302. https://doi.org/10.1016/0009-2541(94)90059-0.
Meyers, P.A., 1997. Organic geochemical proxies of paleoceanographic, paleolimnologic, and paleoclimatic processes. Organic Geochemistry 27 (5–6), 213–250. https://doi.org/10.1016/S0146-6380(97)00049-1.
Meyers, P.A., Lallier-Vergès, E., 1999. Lacustrine sedimentary organic matter records of Late Quaternary paleoclimates. Journal of Paleolimnology 21 (3), 345–372. https://doi.org/10.1023/A:1008073732192.
Morris JT, Barber DC, Callaway JC, Chambers R, Hagen SC, Hopkinson CS, Johnson BJ, Megonigal P, Neubauer SC, Troxler T, Wigand C. 2016. Contributions of organic and inorganic matter to sediment volume and accretion in tidal wetlands at steady state. *Earth's Future*. John Wiley and Sons Inc, 4(4): 110–121. Doi: 10.1002/2015EF000334.
Murdiyarso, D., Purbopuspito, J., Kauffman, J.B., Warren, M.W., Sasmito, S.D., Donato, D.C., Manuri, S., Krisnawati, H., Taberima, S., Kurnianto, S., 2015. The potential of Indonesian mangrove forests for global climate change mitigation. Nature Climate Change 5 (12), 1089–1092. https://doi.org/10.1038/nclimate2734.
Patience, A., 1996. Relationships between organo-mineral supply and early diagenesis in the lacustrine environment: a study of surficial sediments from the Lac du Bouchet (Haute Loire, France). Quaternary Science Reviews 15 (2–3), 213–221. https://doi.org/10.1016/0277-3791(95)00024-0.
Phang, V.X.H., Chou, L.M., Friess, D.A., 2015. Ecosystem carbon stocks across a tropical intertidal habitat mosaic of mangrove forest, seagrass meadow, mudflat and sandbar. *Earth Surface Processes and Landforms*. John Wiley and Sons Ltd 40 (10), 1387–1400. https://doi.org/10.1002/esp.3745.
Ranjan, R.K., Routh, J., Ramanathan, A.L., Klump, J.V., 2011. Elemental and stable isotope records of organic matter input and its fate in the Pichavaram mangrove–estuarine sediments (Tamil Nadu, India). Marine Chemistry 126 (1–4), 163–172. https://doi.org/10.1016/j.marchem.2011.05.005.
Robbins, J.A., 1978. Geochemical and geophysical applications of radioactive lead. *Biogeochemistry of Lead in the Environment*. Elsevier Scientific, pp. 285–393.
Rosentreter, J.A., Maher, D.T., Erler, D.V., Murray, R.H., Eyre, B.D., 2018. Methane emissions partially offset "blue carbon" burial in mangroves. Science Advances 4 (6). https://doi.org/10.1126/sciadv.aao4985.
Rovai, A.S., Twilley, R.R., Castañeda-Moya, E., Riul, P., Cifuentes-Jara, M., Manrow-Villalobos, M., Horta, P.A., Simonassi, J.C., Fonseca, A.L., Pagliosa, P.R., 2018. Global controls on carbon storage in mangrove soils. *Nature Climate Change*. Springer, US 8 (6), 534–538. https://doi.org/10.1038/s41558-018-0162-5.
Rsis, 2024. Área de Protección de Flora y Fauna. Playa Tortuguera El Verde Camacho, Ramsar Sites Information Service.

Sanchez-Cabeza, J.A., Ruiz-Fernández, A.C., 2012. 210Pb sediment radiochronology: An integrated formulation and classification of dating models. Geochimica et Cosmochimica Acta 82, 183–200. https://doi.org/10.1016/j.gca.2010.12.024.

Sebag, D., Copard, Y., Di-Giovanni, C., Durand, A., Laignel, B., Ogier, S., Lallier-Vergès, E., 2006. Palynofacies as useful tool to study origins and transfers of particulate organic matter in recent terrestrial environments: Synopsis and prospects. Earth-Science Reviews 79 (3–4), 241–259. https://doi.org/10.1016/j.earscirev.2006.07.005.

Sebag, D., Verrecchia, E.P., Cécillon, L., Adatte, T., Albrecht, R., Aubert, M., Bureau, F., Cailleau, G., Copard, Y., Decaens, T., Disnar, J.-R., Hetényi, M., Nyilas, T., Trombino, L., 2016. Dynamics of soil organic matter based on new Rock-Eval indices. *Geoderma*. Elsevier b.v. 284, 185–203. https://doi.org/10.1016/j.geoderma.2016.08.025.

Smoak, J.M., Breithaupt, J.L., Smith, T.J., Sanders, C.J., 2013. Sediment accretion and organic carbon burial relative to sea-level rise and storm events in two mangrove forests in Everglades National Park. *Catena*. Elsevier b.v. 104, 58–66. https://doi.org/10.1016/j.catena.2012.10.009.

Soto-Galera, E., Piera, J., López, P., 2010. Spatial and temporal land cover changes in Terminos Lagoon Reserve. Mexico. *Revista De Biologia Tropical* 58 (2), 565–575. https://doi.org/10.15517/rbt.v58i2.5229.

Southward, A.J., Tyler, P.A., Young, C.M., Fuiman, L.A., 2005. Aquatic Geomicrobiology. Elsevier, Amsterdam.

Twilley, R.R., Rovai, A.S., Riul, P., 2018. Coastal morphology explains global blue carbon distributions. Frontiers in Ecology and the Environment 16 (9), 503–508. https://doi.org/10.1002/fee.1937.

Tyson, R.V., 1995. *Sedimentary Organic Matter*. *Sedimentary Organic Matter*. Dordrecht, Springer, Netherlands.

Venegas-Pérez, M.C.Y., 2003. Ficha Informativa de los Humedales de Ramsar (FIR). Laguna de Términos.

Williams, E.K., Rosenheim, B.E., 2015. What happens to soil organic carbon as coastal marsh ecosystems change in response to increasing salinity? An exploration using ramped pyrolysis. *Geochemistry, Geophysics, Geosystems*. Blackwell Publishing Ltd 16 (7), 2322–2335. https://doi.org/10.1002/2015GC005839.

Woodroffe, S.A., Horton, B.P., Larcombe, P., Whittaker, J.E., 2005. Intertidal mangrove foraminifera from the central Great Barrier Reef Shelf, Australia: Implications for sea-level reconstruction. Journal of Foraminiferal Research 35 (3), 259–270. https://doi.org/10.2113/35.3.259.

Yáñez-Arancibia, A., Day, J.W., 2005. Ecosystem functioning: The basis for sustainable management of Terminos Lagoon. Campeche Mexico, Jalapa, Veracruz, Mexico.

Zhang, Y., Fu, H., Yang, X., Liu, Z., 2023. Anthropogenically driven changes to organic matter input in sediments of Lake Chaohu. In: Over the past 166 Years. *Catena*. Elsevier B.V, Eastern China, p. 231. https://doi.org/10.1016/j.catena.2023.107285.